In silico study on anti-Chikungunya virus activity of hesperetin

Adrian Oo [1] , **Pouya Hassandarvish** [1] , **Sek Peng Chin** [2] , **Vannajan Sanghiran Lee** [2] , **Sazaly Abu Bakar** [1] , **Keivan Zandi** Corresp. [1]

[1] Tropical Infectious Disease Research and Education Centre, Department of Medical Microbiology Faculty of Medicine, University of Malaya, Kuala Lumpur, Malaysia

[2] Department of Chemistry, University of Malaya, Kuala Lumpur, Malaysia

Corresponding Author: Keivan Zandi
Email address: keivan@um.edu.my

Background. The re-emerging, *Aedes spp.* transmitted Chikungunya virus (CHIKV) has recently caused large outbreaks in a wide geographical distribution of the world including countries in Europe and America. Though fatalities associated with this self-remitting disease were rarely reported, quality of patients' lives have been severely diminished by polyarthralgia recurrence. Neither effective antiviral treatment nor vaccines are available for CHIKV. Our previous *in vitro* screening showed that hesperetin, a bioflavonoid exhibits inhibitory effect on the virus intracellular replication. Here, we present a study using the computational approach to identify possible target proteins for future mechanistic studies of hesperetin.

Methods. 3D structures of CHIKV nsP2 (3TRK) and nsP3 (3GPG) were retrieved from Protein Data Bank (PDB), whereas nsP1, nsP4 and cellular factor SPK2 were modeled using Iterative Threading Assembly Refinement (I-TASSER) server based on respective amino acids sequence. We performed molecular docking on hesperetin against all four CHIKV non-structural proteins and SPK2. Proteins preparation and subsequent molecular docking were performed using Discovery Studio 2.5 and AutoDock Vina 1.5.6. The Lipinski's values of the ligand were computed and compared with the available data from PubChem. Two non-structural proteins with crystal structures 3GPG and 3TRK in complexed with hesperetin, demonstrated favorable free energy of binding from the docking study, were further explored using molecular dynamics (MD) simulations.

Results. We observed that hesperetin interacts with different types of proteins involving hydrogen bonds, pi-pi effects, pi-cation bonding and pi-sigma interactions with varying binding energies. Among all five tested proteins, our compound has the highest binding affinity with 3GPG at -8.5 kcal/mol. The ligand used in this study also matches the Lipinski's rule of five in addition to exhibiting closely similar properties with that of in PubChem. The docking simulation was performed to obtain a first guess of the binding structure of hesperetin complex and subsequently analysed by MD simulations to assess the reliability of the docking results. Root mean square deviation (RMSD) of the simulated systems from MD simulations indicated that the hesperetin complex remains stable within the simulation timescale.

Discussion. The ligand's tendencies of binding to the important proteins for CHIKV replication were consistent with our previous *in vitro* screening which showed its efficacy in blocking the virus intracellular replication. NsP3 serves as the highest potential target protein for the compound's inhibitory effect, while it is interesting to highlight the possibility of interrupting CHIKV replication via interaction with host cellular factor. By complying the Lipinski's rule of five, hesperetin exhibits drug-like properties which projects its potential as a therapeutic option for CHIKV infection.

1 ***In silico*** study on anti-Chikungunya virus activity of hesperetin

3 Adrian Oo[1], Pouya Hassandarvish[1], Chin Sek Peng[2], Vannajan Sanghiran Lee[2], Sazaly Abu
4 Bakar[1], Keivan Zandi[1]

6 [1] Tropical Infectious Disease Research and Education Centre, Department of Medical

7 Microbiology, Faculty of Medicine, University of Malaya, 50603 Kuala Lumpur, Malaysia.

8 [2] Department of Chemistry, Faculty of Science, University of Malaya, 50603 Kuala Lumpur,

9 Malaysia.

11 **Corresponding author :**

12 Keivan Zandi[1]

25   **Abstract**

26   **Background.** The re-emerging, *Aedes spp.* transmitted Chikungunya virus (CHIKV) has recently

27   caused large outbreaks in a wide geographical distribution of the world including countries in

28   Europe and America. Though fatalities associated with this self-remitting disease were rarely

29   reported, quality of patients' lives have been severely diminished by polyarthralgia recurrence.

30   Neither effective antiviral treatment nor vaccines are available for CHIKV. Our previous *in*

31   *vitro* screening showed that hesperetin, a bioflavonoid exhibits inhibitory effect on the virus

32   intracellular replication. Here, we present a study using the computational approach to identify

33   possible target proteins for future mechanistic studies of hesperetin.

34   **Methods.** 3D structures of CHIKV nsP2 (3TRK) and nsP3 (3GPG) were retrieved from Protein

35   Data Bank (PDB), whereas nsP1, nsP4 and cellular factor SPK2 were modeled using Iterative

36   Threading Assembly Refinement (I-TASSER) server based on respective amino acids sequence.

37   We performed molecular docking on hesperetin against all four CHIKV non-structural proteins

38   and SPK2. Proteins preparation and subsequent molecular docking were performed using

39   Discovery Studio 2.5 and AutoDock Vina 1.5.6. The Lipinski's values of the ligand were

40   computed and compared with the available data from PubChem. Two non-structural proteins with

41   crystal structures 3GPG and 3TRK in complexed with hesperetin, demonstrated favorable free

42   energy of binding from the docking study, were further explored using molecular dynamics (MD)

43   simulations.

44   **Results.** We observed that hesperetin interacts with different types of proteins involving hydrogen

45   bonds, pi-pi effects, pi-cation bonding and pi-sigma interactions with varying binding energies.

46   Among all five tested proteins, our compound has the highest binding affinity with 3GPG at -8.5

47   kcal/mol. The ligand used in this study also matches the Lipinski's rule of five in addition to

48   exhibiting closely similar properties with that of in PubChem. The docking simulation was

49   performed to obtain a first guess of the binding structure of hesperetin complex and subsequently

50   analysed by MD simulations to assess the reliability of the docking results. Root mean square

51   deviation (RMSD) of the simulated systems from MD simulations indicated that the hesperetin

52   complex remains stable within the simulation timescale.

53   **Discussion.** The ligand's tendencies of binding to the important proteins for CHIKV replication

54   were consistent with our previous *in vitro* screening which showed its efficacy in blocking the

55   virus intracellular replication. NsP3 serves as the highest potential target protein for the

56   compound's inhibitory effect, while it is interesting to highlight the possibility of interrupting

57   CHIKV replication via interaction with host cellular factor. By complying the Lipinski's rule of

58   five, hesperetin exhibits drug-like properties which projects its potential as a therapeutic option for

59   CHIKV infection.

60

61

62

63

64

65

66

67

68

Introduction

70   Chikungunya virus (CHIKV) is an arthropod-borne virus classified under the arthritogenic group

71   of *Alphavirus* genus from the *Togaviridae* family (Assunção-Miranda et al. 2013). CHIKV is

72   primarily transmitted by female mosquitoes of the *Aedes* genus, namely *Aedes aegypti* and *Aedes*

73   *albopictus*, though *Culex ethiopicus* and *Anopheles stephensi* have also been reported as potential

74   vectors. Over the years, massive outbreaks have been recorded in Africa, India and Indian Ocean

75   islands as well as South and South-East Asia (Beesoon et al. 2008; Josseran et al. 2006; Lanciotti

76   et al. 2007). In addition to the spread of CHIKV by *Aedes albopictus* to America and Europe,

77   return of high viraemia infected travellers, have caused concerns of CHIKV transmittance to new

78   endemic regions (Angelini et al. 2007; Vega-Rúa et al. 2014). Within 2-4 days following the initial

79   mosquito bite, CHIKV enters the bloodstream where it disseminates to its respective target organs

80   for subsequent replication. Infected patients generally suffer from symptoms such as polythermia

81   (> 39°C), maculopapular rashes, polyarthralgia, cephalgia and nauseas (Taubitz et al. 2007).

82   Further complications involving the inflammation of heart muscles (myocarditis), brain and

83   meninges (meningoencephalitis) as well as haemorrhage have also been reported but rare (Farnon

84   et al. 2008). Though CHIKV is a self-limiting viral infection, 30-40% of patients have been

85   complaining of recurrent joint pains which may last from a few weeks up to several years following

86   recovery (Manimunda et al. 2010).

87   This small, spherical and enveloped virus contains a single positive-strand RNA genome which is

88   about 11.8kb in size (Presti et al. 2014). The genome is made up of two open reading frames

89   (ORFs), whereby the ORF covering 5' two-thirds of the genome codes for the non-structural

90   proteins, whereas CHIKV structural proteins are encoded by the 3' ORF (Snyder et al. 2013).

91   Cleavage of the polyproteins results in five structural (C, E3, E2, 6K, E1) and four nonstructural

92   (nsP1, nsP2, nsP3, nsP4) proteins, with distinct functions.

93   While the structural proteins are mainly involved in the early stages of CHIKV replication cycle

94   comprising of the attachment and entry of virus particles into infected cells, CHIKV nonstructural

95   proteins are vital for the intracellular replication of new virus particles. The nonstructural proteins

96   originated from a polyprotein (P1234) which is directly translated from the 5' two-thirds of

97   CHIKV genomic RNA. The section between nsP3 and nsP4 in the precursor protein is then cleaved

98   in *cis*, resulting in P123 and nsP4 proteins (Merits et al. 2001). Subsequently, an unstable

99   replication complex made up of these proteins as well as cellular factors is assembled, which

100 synthesizes minus-strand genomic RNA. Further cleavage of the P123 protein into nsP1 and P23,

101 together with nsP4, gives rise to a replication complex within virus-induced cytopathic vacuoles

102 (CPV I), capable of both the synthesis of sense and antisense genomic RNA (Froshauer et al. 1988;

103 Salonen et al. 2003; Shirako & Strauss 1994). Following the complete processing into individual

104 nsP1, nsP2, nsP3 and nsP4 proteins, a stable polymerase complex is formed capable of the

105 production of the positive-sense genomic and subgenomic RNA molecules (Lemm et al. 1994).

106 The nsP1 protein via its guanine-7-methyltransferase and guanylyl transferase activities, catalyses

107 the capping and methylation of newly synthesized viral mRNA in addition to its role in the

108 synthesis of viral antisense RNA molecules (Ahola & Kääriäinen 1995; Mi & Stollar 1991). NsP1

109 is also involved in the attachment of virus polymerase complex to cellular membranes through

110 interactions between the negatively-charged phospholipids with the amphipathic binding peptide

111 (BP), and is enhanced by nsP1 palmitoylation (Peränen et al. 1995). Study has shown that alteration

112 in the specific as well as the surrounding palmitoylation site reduces virus replication hence, its

113 viability (Ahola et al. 2000). The nsP2 is multifunctional whereby it possesses the N-terminal RNA

114 triphosphatase domain which catalyses the capping of viral RNA as well as the protein's RNA

115 helicase activity (Fros et al. 2013; Karpe et al. 2011).

116 The C-terminal of the protein has cysteine protease activity which is essential for the autocatalysis

117 of the P123 polyprotein, as well as a domain with methyltransferase-like activity of undiscovered

118 function (Bouraï et al. 2012). It has also been reported that nsP2 regulates the transcription and

119 translation of viral proteins using the host cell machinery besides protection against interferon's

120 inhibitory activity (Fros et al. 2010). The nsP3 protein is made up of three domains, namely the

121 evolutionarily highly conserved N-terminus, the centre domain unique only for *Alphaviruses* and

122 the heavily phosphorylated C-terminus. Its macrodomain is suggested to mediate ADP-ribose 1"-

123 phosphate and/or other ADP-ribose derivatives metabolism which regulate cellular activities

124 (Seyedi et al. 2016). On the other hand, the Cterminus contains Src-homology 3 (SH3) binding

125 motifs for the localization of cellular amphiphysins Amph1 and BIN1/Amph2 following virus

126 infection which promote *Alphavirus* genome replication (Neuvonen et al. 2011). NsP3 also

127 mediates cellular stress response by blocking the assembly of stress granules via the interaction

128 between its SH3 binding motifs with Ras-GAP SH3 domain-binding protein (G3BP) (Fros et al.

129 2012). On the other hand, CHIKV nsP4 functions as RNA-dependent RNA polymerase vital for

130 the elongation of the newly synthesised viral RNA molecules (Rathore et al. 2013). A study also

131 demonstrated the close interactions between CHIKV nsP4 as well as nsP3 proteins with the heat

132 shock protein, HSP-90 which has been shown to play an important role in the replication process

133 of several DNA and RNA viruses (Rathore et al. 2014).

134 Sphingosine kinases (SPKs) are lipid kinases involved in the conversion of sphingosine into

135 sphingosine-1-phosphate (S1P). Two types of SPKs are present in mammalian cells, namely SPK1

136 and SPK2 which are translated from *SPHK1* gene on chromosome 17 and *SPHK2* gene on

137 chromosome 19 respectively (Neubauer & Pitson 2013). Previous studies have shown close

138 association between SPK/S1P pathway and important cellular processes such as cell growth,

139 inflammation and immune responses, with both types of SPKs having the opposing effects

140 (Maceyka et al. 2005; Okada et al. 2005; Olivera et al. 1999; Snider et al. 2010). Interestingly, in

141 addition to its contribution towards the development of degenerative diseases in humans, SPKs

142 also play important roles in several viral infections, including Dengue and Influenza A viruses for

143 SPK1 as well as Hepatitis C virus, Kaposi's sarcoma-associated herpes virus, and most importantly

144 for our study, CHIKV for SPK2 (Clarke et al. 2015; Couttas et al. 2014; Dai et al. 2014; Reid et

145 al. 2015; Seo et al. 2013; Yamane et al. 2014).

146 Flavonoids are a group of polyphenolic plant compounds which are synthesised via the

147 phenylpropanoid pathway. Over the years, different types of flavonoids have been the subject of

148 research for their wide range of medicinal benefits – anti-oxidant, anti-tumour, anti-inflammation

149 and anti-microbial activities (Martínez-Pérez et al. 2016; Paul Dzoyem et al. 2013; Procházková

150 et al. 2011; Serafini et al. 2010). Indeed, various flavonoids have been reported for their antiviral

151 properties against Dengue Virus (DENV), Herpes Simplex Virus

152 (HSV), Human Cytomegalovirus (HCMV) and etc (Cotin et al. 2012; Lyu et al. 2005; Moghaddam

153 et al. 2014; Ono et al. 1989; Zandi et al. 2011). In our previous study, we have found that hesperetin

154 which belongs to the flavanone class of flavonoids possesses effective inhibitory effect on the *in*

155 *vitro* intracellular replication of CHIKV (unpublished data). Hence, at present we will be

156 performing an *in silico* investigation to identify the possible target proteins for subsequent

157 mechanistic study of hesperetin on CHIKV.

158

Materials and Methods

Receptor and ligand preparation

161   The receptors used in this study are the three-dimensional protein structures of CHIKV nsP1, nsP2,

162   nsP3, nsP4 and the mammalian cells' SPK2. CHIKV nsP1 and nsP4 as well as the SPK2 protein

163   structures were modelled using the Iterative Threading Assembly Refinement (ITASSER) server

164   based on the amino acid sequences obtained from Universal Protein Resource (UniProt) (Roy et

165   al. 2010; Yang et al. 2015; Zhang 2008). On the other hand, nsP2 and nsP3 crystal structures were

166   retrieved from the Protein Data Bank (PDB) with PDB IDs of 3TRK and 3GPG respectively. Using

167   the Discovery Studio 2.5 software, water molecules were removed and CHARMM27 force field

168   was applied onto these protein structures. Subsequently, steric overlaps were removed and the

169   structures were processed 1000 steps using the smart-minimizer algorithm. Hesperetin was used

170   as the ligand in this experiment, of which the ligand structure was generated using ChemDraw

171   software (CambridgeSoft). The 2D-structure was then minimized using the Discovery Studio 2.5

172   software followed by the preparation of both the ligand and receptors during which hydrogen

173   molecules were added using the AutoDock Vina 1.5.6 software, which were then saved as PDBQT

174   files.

Molecular Docking

176   In our study, the binding properties of the ligand to each protein were analysed using the AutoDock

177   Vina 1.5.6 software. Blind dockings were performed in which grid boxes of sizes sufficient to

178   cover the entire receptors of interest were constructed according to the parameters as tabulated in

179   Table 1. All grid boxes were formed at spacing size of 1.000 Å. Following the docking procedure,

180 the resulting PDBQT output file was first opened in the PyMOL software in which all protein

181 conformations were converged in a single file for further analysis. Each conformation was then

182 analysed using the AutoDock Vina 1.5.6 and Discovery Studio 2.5 software whereby information

183 such as binding affinities, interaction energies, van der Waals energies, electrostatic energies,

184 hydrogen bonding, pi-pi interactions, pi-cation interactions and close contacting residues were

185 obtained and recorded. Separately, the Lipinski's values for hesperetin were determined using the

186 Lipinski Filters (SCFBio, Delhi) (Jayaram et al. 2012; Lipinski 2004).

187 **Molecular dynamics simulations**
188
189 The docked complexes of hesperetin to the non-structural proteins – 3GPG and 3TRK which

190 demonstrated favourable free energy of binding during molecular docking were used as starting

191 structures for the molecular dynamics (MD) simulations. A total of 10 ns MD simulations were

192 performed using AMBER 14 (Case et al. 2010). Amber ff14SB force field (Maier et al. 2015) was

193 used to describe the proteins, waters and counter-ions. Antechamber was used to determine GAFF

194 atom types for hesperetin, following Amber standard protocol. Restrained ElectroStatic Potential

195 (RESP) charges were employed for ligands (Bayly et al. 1993). MD simulations were performed

196 using constant pressure (P) and temperature (T), NPT ensemble, maintaining the pressure and

197 temperature at 1.0 atm and 310 K, respectively, by means of anisotropic pressure scaling and

198 Langevin dynamics. The periodic boundary conditions based on the particle mesh Ewald method

199 with a non-bonded cutoff of 8 Å were used. The integration time step was set at 2 fs and the

200 SHAKE algorithm was used to constrain bond lengths involving hydrogen atoms. The system

201 simulated underwent two stages of minimization using steepest descent and conjugate gradient

202 with different parts of the system gradually released in stages. Then, it was slowly heated from 0

203 to 310 K within 500 ps with restraints on the complex. After the heating stage, the system was

204   equilibrated for 1 ns, followed by another 10 ns of a relaxed MD run. The complete system

205   trajectory was collected every 2 ps for analysis. Trajectories analyses were performed using the

206   CPPTRAJ modules (Roe & Cheatham 2013) of AMBER 16. The relative binding free energy for

207   the complex was evaluated using MM-GBSA approach as implemented in Amber, using

208   MMPBSA.py module (Miller et al. 2012) in Amber 16. A total of 500 snapshots from the relax

209   MD trajectories were included in the calculations.

210

211   **Results**

212   In this study, hesperetin was screened for potential inhibitory activities against all four CHIKV's

213   non-structural proteins, namely nsP1, nsP2, nsP3 and nsP4 in addition to SPK2 via the docking of

214   the compound to each protein. **Figures 1A-E** show the bindings of hesperetin with the highest

215   binding affinities upon docking against the proteins of interest. As illustrated, hesperetin exhibits

216   the strongest binding affinity against 3GPG (-8.5 kcal/mol), followed by nsP4 and SPK2 (-7.7

217   kcal/mol), nsP1 (-7.6 kcal/mol) and finally 3TRK (-6.9 kcal/mol). The total interaction energies

218   between the ligand and proteins resulting from the electrostatic as well as the weaker van der Waals

219   forces are as tabulated in **Table 2**.

220   Besides looking into the binding affinities and energies involved in the interaction of hesperetin

221   with all five proteins, we have also taken into record of the bonds formed between the ligand and

222   the binding sites on each protein. For nsP1, hydrogen bonds observed between this ligand-receptor

223   proteins interactions are recorded in **Table 3**. Hesperetin exhibits pi-pi and pi-cation interactions

224   with TYR185, PHE43 and ARG70, ARG252, LYS442 respectively **(Table 8)**. The Discovery

225   Studio 2.5 shows close amino acid residues found in the binding pocket between hesperetin and

226   nsP1, namely LEU15, ALA17, LEU18, GLN19, ALA21, TYR22, ASN39, ALA40, PHE43,

227   ALA40, PRO68, ALA69, ARG70, ARG71 and ALA104 as displayed in **Figure 2**.

228   CHIKV's nsP2 is an important protein for the initial stage of new viral RNA synthesis. In this

229   study we carried out molecular docking of hesperetin on the cysteine protease domain of the virus

230   nsP2, as denoted as 3TRK. The hydrogen bonds between hesperetin and 3TRK are as shown in

231   **Table 4**. Pi-effects are observed at tyrosine residues of TYR1079 and TYR1177 as well as the

232   phenylalanine PHE1225 **(Table 8)**. In **Figure 3**, we have demonstrated the close residues of 3TRK

233   with hesperetin at ALA1046, TYR1047, SER1048, TYR1079, ASN1082, LEU1206, GLN1241

234   and GLY1245.

235   Another protein studied is the nsP3 protein as denoted 3GPG, which plays multiple roles in the

236   virus life cycle.. **Table 5** documents the hydrogen bonds linking hesperetin and 3GPG obtained

237   from our docking experiment. Interestingly, we also observed pi-pi interactions with TRP148 and

238   TYR63, pi-cation interaction with LYS118 as well as pi-sigma with GLY30 and VAL113 **(Table**

239   **8)**. Amino acid residues ALA22, ALA23, ASN24, ASP31, GLY32, VAL33, CYS34, PRO107,

240   LEU109, THR111, GLY112, VAL113, TYR114, CYS 143, ARG144 and ASP145 were also found

241   closely in the binding pocket with hesperetin **(Figure 4).**

242   We studied the potential inhibitory activity of hesperetin against CHIKV's nsP4 which serve as

243   the polymerase for the elongation of newly synthesised RNA strands by simulating the docking

244   process of the compound against this protein. In addition to the hydrogen bonds as shown in **Table**

245   **6**, most pi interactions formed in this ligand-protein pair are pi-cations at ARG374 and ARG70

246   **(Table 8)**. The remaining pi-pi interactions formed at TYR22 and

247 TYR185, whereas pi-sigma interaction was observed at ARG70 **(Table 8)**. Illustrated in **Figure 5**

248 are the close residues including TRP199, ALA200, LEU313, CYS315, LYS316, Val321, VAL326,

249 PHE328, ASN363, ILE366, THR372, GLN373.

250 In addition to the virus proteins, we have also docked our compound of interest to cellular factor

251 vital for virus replication such as SPK2. Our work shows hydrogen bonds between hesperetin and

252 SPK2 as tabulated in **Table 7**. TYR372 and ARG351 interact with the ligand via pi-pi and pi-

253 cation bonding respectively **(Table 8)**. The hesperetin-SPK2 interaction also saw amino acid

254 residues such as HIS251, ASN255, ASP259, CYS329, LEU425, PRO426, LEU427, PRO428,

255 LEU432, ALA433, GLU624, GLN625, VAL626, GLU627 and TYR628 in close vicinities within

256 the binding pocket **(Figure 6)**.

257 In order to ensure that the designed hesperetin molecule used in this experiment possesses the

258 necessary drug-like properties to be developed as a therapeutic option for CHIKV infections, the

259 Lipinski's values of our compound were determined and compared with the available data in

260 PubChem **(Table 9)**.

261 Hesperetin was found to bind and remain in the binding site throughout the simulation (see movie

262 files in Supplemental Files section). For both systems (3GPG and 3TRK), root mean square

263 deviation (RMSD) computed using the backbone atoms of the complex with respect to the

264 minimized starting structure was found to be less than 1.8 Å (Figure 7). This showed that the

265 systems are well equilibrated and do not deviate greatly from their initial starting structure. The

266 lowest energy structures of the complexes are shown in Figure 8. To explore the binding of

267 hesperetin to 3GPG and 3TRK, the relative free energy of binding was computed from enthalpy

268 contributions, using snapshots extracted from the trajectories, following the MM-GBSA approach

269 (Kollman et al. 2000; Srinivasan et al. 1998). Table 10 lists the contributions to the binding free

270   energy for the simulated complexes - favourable contributions to the binding arose from van der

271   Waals interactions and the non-polar part of the solvation free energy, as opposed to unfavourable

272   total electrostatic contributions (EEL+EGB). The favourable binding free energy of -28.18 and -

273   17.46 kcal/mol were for 3GPG-hesperetin and 3TRK-hesperetin, respectively. The estimated

274   binding free energy calculated is in agreement with the docking study.

275

Discussion

277   Since the initial Tanzania outbreak in 1952, CHIKV epidemics have been recorded in several parts

278   of the world with different climate systems. The spread of CHIKV to countries outside the tropical

279   regions has been attributed to the single amino acid alteration from alanine to valine (A226V) in

280   the E1 gene (Tsetsarkin et al. 2007). To date, approved therapeutic options and vaccines for

281   CHIKV infections are lacking, though cases of CHIKV infected patients are constantly on the rise

282   globally. Mechanistic studies in the past have shown anti-CHIKV effect of several compounds as

283   a result of their interactions with different viral proteins, hence inhibiting further CHIKV

284   replication (Delogu et al. 2011; Kaur et al. 2013; Lani et al. 2015). Furthermore, computational

285   approaches have been applied by researchers in identifying potential interactions between drug

286   candidates with specific CHIKV proteins in an effort to discover a novel anti-Chikungunya

287   treatment (Agarwal et al. 2015; Nguyen et al. 2014; Singh et al. 2012). In this study, we aim to

288   investigate the potential inhibitory effects of hesperetin, a flavanone, on different CHIVK non-

289   structural proteins in addition to one of the cellular factors vital for CHIKV replication, SPK2.

290
291   Our findings showed that hesperetin possesses interactions with all four CHIKV non-structural

292   proteins as well as SPK2 at different binding affinities. This is consistent with the inhibitory

293   efficacy of hesperetin during the virus intracellular replication observed during our previous *in*

294   *vitro* screening (unpublished data). Hesperetin has the highest tendency to bind with 3GPG

295   with the affinity of -8.5 kcal/mol, followed by both nsp4 and SPK2 at -7.7 kcal/mol, nsP1 with

296   the binding strength of -7.6 kcal/mol and finally 3TRK bound at -6.9 kcal/mol. Hence,

297   CHIKV's nsP3 or 3GPG has the highest potential to be the target protein for hesperetin's

298   inhibitory activity on the virus intracellular replication, though other proteins under study

299   should not be excluded of the possibilities. Interestingly, CHIKV nsP3 protein plays a vital role

300   in the early stages of viral genome replication involving synthesis of viral negative-strand and

301   subgenomic RNAs (Lani et al. 2015). Previous study has also found that mutations resulting in

302   alteration of the protein's amphiphysin SH3 binding motif and downregulation of Amph2

303   expression have been found to diminish *in vitro* viral RNA replication (Neuvonen et al. 2011).

304   Inhibition of both the nsP3 and nsP4 proteins could also block CHIKV replication via the heat

305   shock protein, HSP-90 pathway (Rathore et al. 2014). Besides the virus polymerase nsP4 which

306   also modulate host immune response towards CHIKV infections via the PKR-like ER resident

307   kinase (PERK) pathway (Rathore et al. 2013), the host factor SPK2 was also ranked second by

308   the AutoDock Vina 1.5.6 based on their binding affinities. NsP3-mediated SPK2 re-localisation

309   to a puncta in the cytoplasm following an infection suggested the involvement of SPK2 in

310   CHIKV replication. Close association of SPK2 with host proteins for mRNA processing and

311   gene expression further link SPK2 with CHIKV replication process (Reid et al. 2015). Our

312   findings suggest that inhibitory effect of hesperetin could be contributed by both direct activity

313   on the virus proteins as well as cellular factors vital for the virus replication.

314

315   We have also identified the different types of non-covalent bonds between the ligand and the

316   receptor proteins, including the hydrogen bonds, pi-pi, pi-cation and pi-sigma interactions.

317 Hydrogen bond is a dipole-dipole interaction involving the transfer of a proton from one

318 molecule to the electronegative recipient atom on another molecule. Hydrogen bond varies in

319 strength based on the distance of the hydrogen bond, whereby as described by Szatylowicz,

320 hydrogen bonds are classified as strong, moderate and weak if they fall into the ranges of 1.2 Å

321 -1.5 Å, 1.5 Å -2.2 Å and >2.2 Å respectively (Szatyłowicz 2008). None of the hydrogen bonds

322 formed between hesperetin and all five proteins in this study fall under the strong category.

323 Instead, hesperetin formed moderately strong hydrogen bonds with relatively strong binding

324 affinities with ASP310, GLY311, ASP36, ARG71 and LEU135 of nsP1, TYR142, LEU108,

325 SER110, ARG144, GLU17, THR122 and ASN72 of 3GPG, GLN364, ALA104, ALA103,

326 ARG110, LEU135, ASP479 and THR437 of nsP4, and finally ARG373, GLN625 and ASP342

327 of SPK2. Though strong hydrogen bonds were also observed between hesperetin and 3TRK at

328 ASP1246 and TRP1084, their binding affinities were the lowest relative to the other four

329 proteins studied.

330 Another type of non-covalent interaction investigated in this experiment are the pi interactions,

331 which involve the electron-rich pi-system with another pi-system, anion, cation or other

332 molecules. Among all the pi-interactions investigated in this study, the pi-sigma bonds have the

333 strongest binding strength due to the larger overlaps of its s-orbitals (Harmony 1990; Sinanoglu

334 & Wiberg 1963). From our findings, we observed four pi-sigma interactions between hesperetin

335 and 3TRK at PHE1225, 3GPG at GLY30 and VAL113 as well as ARG70 of nsP4. We have

336 also documented the strong electrostatic forces between a polarised ligand and a receptor's

337 binding site, as well as the van der Waals interaction energies. Van der Waals interactions,

338 which are generally weaker as compared with the other forces, are formed when the cationic

339 nucleus of a molecule is attracted to the electron cloud of another molecule, or vice versa. It

340 results from transient alterations of polarisation in the nucleus affecting the surrounding dipole-

341 dipole interactions and the nearby electron distribution. The weak van der Waals are

342 complemented with the presence of large numbers of bindings arising from good electrostatic

343 and steric interactions between both molecules (Copeland 2013).

344 The Lipinski's Rule of Five, also known as the Pfizer's Rule of Five by Christopher A. Lipinski

345 explains the basic criteria which one compound needs to possess to exhibit druglikeness properties.

346 Compounds which fulfil the following requirements are most likely to be membrane permeable

347 and have high bioavailability following oral administration – molecular weight less than 500

348 g/mol, Log P less than 5, less than 5 H-bond donors, less than 10 H-bond acceptors and molar

349 refractivity in the range of 40-130 (Lipinski et al. 2012). As shown in **Table 9**, the hesperetin

350 molecule used in our study matches all five of the Lipinski's Rule of Five – molecular weight of

351 302 g/mol, Log P of 2.5, 3 H-bond donors, 6 H-bond acceptors and molar refractivity of 76.75.

352 We compared our findings with the available data from PubChem to ensure that the ligand

353 designed is reliable for our docking experiment. The results suggest that hesperetin has the

354 necessary properties to be developed into an effective oral therapeutic for CHIKV infections.

355 Furthermore, the non-structural proteins (3GPG and 3TRK) in complexed with hesperetin

356 remained stable throughout the 10 ns MD simulations. In all, these findings are of utmost

357 importance for determining whether hesperetin has the potential to be developed into an effective

358 antiviral drug against CHIKV infections as well as its highest possible target protein.

359

360 **Conclusion**

361 Hesperetin possesses interactions with all four CHIKV non-structural proteins in addition to SPK2

362 which plays a role in the virus replication cycle. These findings enhance our understandings on the

363   possible underlying inhibitory mechanism of CHIKV replication, hence allowing further studies

364   on these target proteins for the development of novel anti-CHIKV drug.

365

366   **References**

367   Agarwal T, Asthana S, and Bissoyi A. 2015. Molecular modeling and docking study to elucidate
368   novel chikungunya virus nsP2 protease inhibitors. *Indian journal of pharmaceutical*
369   *sciences* 77:453.
370

371   Ahola T, and Kääriäinen L. 1995. Reaction in alphavirus mRNA capping: formation of a
372   covalent complex of nonstructural protein nsP1 with 7-methyl-GMP. *Proceedings of the*
373   *National Academy of Sciences* 92:507-511.
374

375   Ahola T, Kujala P, Tuittila M, Blom T, Laakkonen P, Hinkkanen A, and Auvinen P. 2000.
376   Effects of palmitoylation of replicase protein nsP1 on alphavirus infection. *Journal of*
377   *virology* 74:6725-6733.
378

379   Angelini R, Finarelli A, Angelini P, Po C, Petropulacos K, Macini P, Fiorentini C, Fortuna C,
380   Venturi G, and Romi R. 2007. An outbreak of chikungunya fever in the province of
381   Ravenna, Italy. *Euro Surveill* 12:E070906.
382

383   Assunção-Miranda I, Cruz-Oliveira C, and Da Poian AT. 2013. Molecular mechanisms involved
384   in the pathogenesis of alphavirus-induced arthritis. *BioMed research international* 2013.
385

386   Bayly CI, Cieplak P, Cornell W, and Kollman PA. 1993. A well-behaved electrostatic potential
387   based method using charge restraints for deriving atomic charges: the RESP model. *The*
388   *Journal of Physical Chemistry* 97:10269-10280.
389

390   Beesoon S, Funkhouser E, Kotea N, Spielman A, and Robich RM. 2008. Chikungunya fever,
391   Mauritius, 2006. *Emerging infectious diseases* 14:337.
392

393   Bouraï M, Lucas-Hourani M, Gad HH, Drosten C, Jacob Y, Tafforeau L, Cassonnet P, Jones
394   LM, Judith D, and Couderc T. 2012. Mapping of Chikungunya virus interactions with
395   host proteins identified nsP2 as a highly connected viral component. *Journal of virology*
396   86:3121-3134.
397

398   Case DA, Babin V, Berryman J, Betz RM, Cai Q, Cerutti DS, Cheatham III TE, Darden TA,
399   Duke RE, Gohlke H, Goetz AW, Gusarov S, Homeyer N, Janowski P, Kaus J,
400   Kolossváry I, Kovalenko A, Lee TS, LeGrand S, Luchko T, Luo R, Madej B, Merz KM,
401   Paesani F, Roe DR, Roitberg A, Sagui C, Salomon-Ferrer R, Seabra G, Simmerling CL,
402   Smith W, Swails J, Walker RC, Wang J, Wolf RM, Wu X, and Kollman PA. 2010.
403   AMBER 14, University of California, San Francisco.
404

405 Clarke JN, Davies LK, Calvert JK, Gliddon BL, Al Shujari WH, Aloia AL, Helbig KJ, Beard
406   MR, Pitson SM, and Carr JM. 2015. Reduction in sphingosine kinase 1 influences the
407   susceptibility to dengue virus infection by altering anti-viral responses. *Journal of*
408   *General Virology*.
409

410 Copeland RA. 2013. *Evaluation of enzyme inhibitors in drug discovery: a guide for medicinal*
411   *chemists and pharmacologists*: John Wiley & Sons.
412

413 Cotin S, Calliste C-A, Mazeron M-C, Hantz S, Duroux J-L, Rawlinson WD, Ploy M-C, and
414   Alain S. 2012. Eight flavonoids and their potential as inhibitors of human
415   cytomegalovirus replication. *Antiviral research* 96:181-186.
416

417 Couttas TA, Kain N, Daniels B, Lim XY, Shepherd C, Kril J, Pickford R, Li H, Garner B, and
418   Don AS. 2014. Loss of the neuroprotective factor Sphingosine 1-phosphate early in
419   Alzheimer's disease pathogenesis. *Acta neuropathologica communications* 2:1.
420

421 Dai L, Plaisance-Bonstaff K, Voelkel-Johnson C, Smith CD, Ogretmen B, Qin Z, and Parsons C.
422   2014. Sphingosine kinase-2 maintains viral latency and survival for KSHV-infected
423   endothelial cells. *PloS one* 9.
424

425 Delogu I, Pastorino B, Baronti C, Nougairède A, Bonnet E, and de Lamballerie X. 2011. In vitro
426   antiviral activity of arbidol against Chikungunya virus and characteristics of a selected
427   resistant mutant. *Antiviral research* 90:99-107.
428

429 Farnon EC, Sejvar JJ, and Staples JE. 2008. Severe disease manifestations associated with acute
430   chikungunya virus infection*. *Critical care medicine* 36:2682-2683.
431

432 Fros JJ, Domeradzka NE, Baggen J, Geertsema C, Flipse J, Vlak JM, and Pijlman GP. 2012.
433   Chikungunya virus nsP3 blocks stress granule assembly by recruitment of G3BP into
434   cytoplasmic foci. *Journal of virology* 86:10873-10879.
435

436 Fros JJ, Liu WJ, Prow NA, Geertsema C, Ligtenberg M, Vanlandingham DL, Schnettler E, Vlak
437   JM, Suhrbier A, and Khromykh AA. 2010. Chikungunya virus nonstructural protein 2
438   inhibits type I/II interferon-stimulated JAK-STAT signaling. *Journal of virology*
439   84:10877-10887.
440

441 Fros JJ, van der Maten E, Vlak JM, and Pijlman GP. 2013. The C-terminal domain of
442   chikungunya virus nsP2 independently governs viral RNA replication, cytopathicity, and
443   inhibition of interferon signaling. *Journal of virology* 87:10394-10400.
444

445 Froshauer S, Kartenbeck J, and Helenius A. 1988. Alphavirus RNA replicase is located on the
446   cytoplasmic surface of endosomes and lysosomes. *The Journal of cell biology* 107:2075-
447   2086.
448

449 Harmony MD. 1990. The equilibrium carbon–carbon single-bond length in ethane. *The Journal*
450   *of chemical physics* 93:7522-7523.
451

452 Jayaram B, Singh T, Mukherjee G, Mathur A, Shekhar S, and Shekhar V. 2012. Sanjeevini: a
453   freely accessible web-server for target directed lead molecule discovery. *BMC*
454   *bioinformatics* 13:S7.
455

456 Josseran L, Paquet C, Zehgnoun A, Caillere N, Le Tertre A, Solet J-L, and Ledrans M. 2006.
457   Chikungunya disease outbreak, Reunion island. *Emerging infectious diseases* 12:1994.
458

459 Karpe YA, Aher PP, and Lole KS. 2011. NTPase and 5′-RNA triphosphatase activities of
460   Chikungunya virus nsP2 protein. *PloS one* 6:e22336.
461

462 Kaur P, Thiruchelvan M, Lee RCH, Chen H, Chen KC, Ng ML, and Chu JJH. 2013. Inhibition of
463   chikungunya virus replication by harringtonine, a novel antiviral that suppresses viral
464   protein expression. *Antimicrobial agents and chemotherapy* 57:155167.
465

466 Kollman PA, Massova I, Reyes C, Kuhn B, Huo S, Chong L, Lee M, Lee T, Duan Y, Wang W,
467   Donini O, Cieplak P, Srinivasan J, Case DA, and Cheatham TE. 2000. Calculating
468   structures and free energies of complex molecules: combining molecular mechanics and
469   continuum models. *Accounts of chemical research* 33:889-897.
470

471 Lanciotti RS, Kosoy OL, Laven JJ, Panella AJ, Velez JO, Lambert AJ, and Campbell GL. 2007.
472   Chikungunya virus in US travelers returning from India, 2006. *Emerging infectious*
473   *diseases* 13:764.
474

475 Lani R, Hassandarvish P, Chiam CW, Moghaddam E, Chu JJH, Rausalu K, Merits A, Higgs S,
476   Vanlandingham D, and Bakar SA. 2015. Antiviral activity of silymarin against
477   chikungunya virus. *Scientific reports* 5.
478

479 Lemm JA, Rümenapf T, Strauss EG, Strauss JH, and Rice C. 1994. Polypeptide requirements for
480   assembly of functional Sindbis virus replication complexes: a model for the temporal
481   regulation of minus-and plus-strand RNA synthesis. *The EMBO journal* 13:2925.
482

483 Lipinski CA. 2004. Lead-and drug-like compounds: the rule-of-five revolution. *Drug Discovery*
484   *Today: Technologies* 1:337-341.
485

486 Lipinski CA, Lombardo F, Dominy BW, and Feeney PJ. 2012. Experimental and computational
487   approaches to estimate solubility and permeability in drug discovery and development
488   settings. *Advanced drug delivery reviews* 64:4-17.
489

490 Lyu S-Y, Rhim J-Y, and Park W-B. 2005. Antiherpetic activities of flavonoids against herpes
491   simplex virus type 1 (HSV-1) and type 2 (HSV-2) in vitro. *Archives of pharmacal*
492   *research* 28:1293-1301.

493

494   Maceyka M, Sankala H, Hait NC, Le Stunff H, Liu H, Toman R, Collier C, Zhang M, Satin LS,
495   and Merrill AH. 2005. SphK1 and SphK2, sphingosine kinase isoenzymes with opposing
496   functions in sphingolipid metabolism. *Journal of Biological Chemistry* 280:37118-37129.
497

498   Maier JA, Martinez C, Kasavajhala K, Wickstrom L, Hauser KE, and Simmerling C. 2015.
499   ff14SB: Improving the Accuracy of Protein Side Chain and Backbone Parameters from
500   ff99SB. *J Chem Theory Comput* 11:3696-3713. 10.1021/acs.jctc.5b00255
501

502   Manimunda SP, Vijayachari P, Uppoor R, Sugunan AP, Singh SS, Rai SK, Sudeep AB,
503   Muruganandam N, Chaitanya IK, and Guruprasad DR. 2010. Clinical progression of
504   chikungunya fever during acute and chronic arthritic stages and the changes in joint
505   morphology as revealed by imaging. *Transactions of the Royal Society of Tropical*
506   *Medicine and Hygiene* 104:392-399.
507

508   Martínez-Pérez C, Ward C, Turnbull AK, Mullen P, Cook G, Meehan J, Jarman EJ, Thomson PI,
509   Campbell CJ, and McPhail D. 2016. Antitumour activity of the novel flavonoid Oncamex
510   in preclinical breast cancer models. *British Journal of Cancer* 114:905-916.
511

512   Merits A, Vasiljeva L, Ahola T, Kääriäinen L, and Auvinen P. 2001. Proteolytic processing of
513   Semliki Forest virus-specific non-structural polyprotein by nsP2 protease. *Journal of*
514   *General Virology* 82:765-773.
515

516   Mi S, and Stollar V. 1991. Expression of Sindbis virus nsP1 and methyltransferase activity
517   inEscherichia coli. *Virology* 184:423-427.
518

519   Miller BR, McGee TD, Swails JM, Homeyer N, Gohlke H, and Roitberg AE. 2012.
520   MMPBSA.py: An Efficient Program for End-State Free Energy Calculations. *Journal of*
521   *Chemical Theory and Computation* 8:3314-3321. 10.1021/ct300418h
522

523   Moghaddam E, Teoh B-T, Sam S-S, Lani R, Hassandarvish P, Chik Z, Yueh A, Abubakar S, and
524   Zandi K. 2014. Baicalin, a metabolite of baicalein with antiviral activity against dengue
525   virus. *Scientific reports* 4.
526

527   Neubauer HA, and Pitson SM. 2013. Roles, regulation and inhibitors of sphingosine kinase 2.
528   *FEBS Journal* 280:5317-5336.
529

530   Neuvonen M, Kazlauskas A, Martikainen M, Hinkkanen A, Ahola T, and Saksela K. 2011. SH3
531   domain-mediated recruitment of host cell amphiphysins by alphavirus nsP3 promotes
532   viral RNA replication. *PLoS Pathog* 7:e1002383.
533

534   Nguyen PT, Yu H, and Keller PA. 2014. Discovery of in silico hits targeting the nsP3 macro
535   domain of chikungunya virus. *Journal of Molecular modeling* 20:1-12.
536

537 Okada T, Ding G, Sonoda H, Kajimoto T, Haga Y, Khosrowbeygi A, Gao S, Miwa N, Jahangeer
538   S, and Nakamura S-i. 2005. Involvement of N-terminal-extended form of sphingosine
539   kinase 2 in serum-dependent regulation of cell proliferation and apoptosis. *Journal of*
540   *Biological Chemistry* 280:36318-36325.
541
542 Olivera A, Kohama T, Edsall L, Nava V, Cuvillier O, Poulton S, and Spiegel S. 1999.
543   Sphingosine kinase expression increases intracellular sphingosine-1-phosphate and
544   promotes cell growth and survival. *The Journal of cell biology* 147:545-558.
545
546 Ono K, Nakane H, Fukushima M, Chermann J-C, and Barré-Sinoussi F. 1989. Inhibition of
547   reverse transcriptase activity by a flavonoid compound, 5, 6, 7-trihydroxyflavone.
548   *Biochemical and biophysical research communications* 160:982-987.
549
550 Paul Dzoyem J, Hamamoto H, Ngameni B, Tchaleu Ngadjui B, and Sekimizu K. 2013.
551   Antimicrobial action mechanism of flavonoids from Dorstenia species. *Drug discoveries*
552   *& therapeutics* 7:66-72.
553
554 Peränen J, Laakkonen P, Hyvönen M, and Kääriäinen L. 1995. The alphavirus replicase protein
555   nsP1 is membrane-associated and has affinity to endocytic organelles. *Virology* 208:610-
556   620.
557
558 Presti AL, Lai A, Cella E, Zehender G, and Ciccozzi M. 2014. Chikungunya virus,
559   epidemiology, clinics and phylogenesis: A review. *Asian Pacific journal of tropical*
560   *medicine* 7:925-932.
561
562 Procházková D, Boušová I, and Wilhelmová N. 2011. Antioxidant and prooxidant properties of
563   flavonoids. *Fitoterapia* 82:513-523.
564
565 Rathore AP, Haystead T, Das PK, Merits A, Ng M-L, and Vasudevan SG. 2014.
566   Chikungunya virus nsP3 & nsP4 interacts with HSP-90 to promote virus replication:
567   HSP-90 inhibitors reduce CHIKV infection and inflammation in vivo. *Antiviral research*
568   103:7-16.
569
570 Rathore AP, Ng M-L, and Vasudevan SG. 2013. Differential unfolded protein response during
571   Chikungunya and Sindbis virus infection: CHIKV nsP4 suppresses eIF2α
572   phosphorylation. *Virology journal* 10:1.
573
574 Reid SP, Tritsch SR, Kota K, Chiang C-Y, Dong L, Kenny T, Brueggemann EE, Ward MD,
575   Cazares LH, and Bavari S. 2015. Sphingosine kinase 2 is a chikungunya virus host factor
576   co-localized with the viral replication complex. *Emerging microbes & infections* 4:e61.
577
578 Roe DR, and Cheatham TE. 2013. PTRAJ and CPPTRAJ: Software for Processing and Analysis
579   of Molecular Dynamics Trajectory Data. *Journal of Chemical Theory and Computation*
580   9:3084-3095. 10.1021/ct400341p
581

582 Roy A, Kucukural A, and Zhang Y. 2010. I-TASSER: a unified platform for automated protein
583   structure and function prediction. *Nature protocols* 5:725-738.

584

585 Salonen A, Vasiljeva L, Merits A, Magden J, Jokitalo E, and Kääriäinen L. 2003. Properly folded
586   nonstructural polyprotein directs the Semliki Forest virus replication complex to the
587   endosomal compartment. *Journal of virology* 77:1691-1702.

588

589 Seo Y-J, Pritzl CJ, Vijayan M, Bomb K, McClain ME, Alexander S, and Hahm B. 2013.
590   Sphingosine kinase 1 serves as a pro-viral factor by regulating viral RNA synthesis and
591   nuclear export of viral ribonucleoprotein complex upon influenza virus infection. *PloS*
592   *one* 8:e75005.

593

594 Serafini M, Peluso I, and Raguzzini A. 2010. Flavonoids as anti-inflammatory agents.
595   *Proceedings of the Nutrition Society* 69:273-278.

596

597 Seyedi SS, Shukri M, Hassandarvish P, Oo A, Muthu SE, Abubakar S, and Zandi K. 2016.
598   Computational Approach Towards Exploring Potential Anti-Chikungunya Activity of
599   Selected Flavonoids. *Scientific reports* 6.

600

601 Shirako Y, and Strauss JH. 1994. Regulation of Sindbis virus RNA replication: uncleaved P123
602   and nsP4 function in minus-strand RNA synthesis, whereas cleaved products from P123
603   are required for efficient plus-strand RNA synthesis. *Journal of virology* 68:1874-1885.

604

605 Sinanoglu O, and Wiberg KB. 1963. Sigma molecular orbital theory. *Chem Phys* 39:20.

606

607 Singh KD, Kirubakaran P, Nagarajan S, Sakkiah S, Muthusamy K, Velmurgan D, and
608   Jeyakanthan J. 2012. Homology modeling, molecular dynamics, e-pharmacophore
609   mapping and docking study of Chikungunya virus nsP2 protease. *Journal of Molecular*
610   *modeling* 18:39-51.

611

612 Snider AJ, Gandy KAO, and Obeid LM. 2010. Sphingosine kinase: role in regulation of
613   bioactive sphingolipid mediators in inflammation. *Biochimie* 92:707-715.

614

615 Snyder JE, Kulcsar KA, Schultz KL, Riley CP, Neary JT, Marr S, Jose J, Griffin DE, and Kuhn
616   RJ. 2013. Functional characterization of the alphavirus TF protein. *Journal of virology*
617   87:8511-8523.

618

619 Srinivasan J, Cheatham TE, Cieplak P, Kollman PA, and Case DA. 1998. Continuum Solvent
620   Studies of the Stability of DNA, RNA, and Phosphoramidate−DNA Helices. *Journal of*
621   *the American Chemical Society* 120:9401-9409. 10.1021/ja981844+

622

623 Szatyłowicz H. 2008. Structural aspects of the intermolecular hydrogen bond strength: Hbonded
624   complexes of aniline, phenol and pyridine derivatives. *Journal of Physical Organic*
625   *Chemistry* 21:897-914.

626

627 Taubitz W, Cramer JP, Kapaun A, Pfeffer M, Drosten C, Dobler G, Burchard GD, and Löscher
628  T. 2007. Chikungunya fever in travelers: clinical presentation and course. *Clinical*
629  *infectious diseases* 45:e1-e4.

630

631 Tsetsarkin KA, Vanlandingham DL, McGee CE, and Higgs S. 2007. A single mutation in
632  chikungunya virus affects vector specificity and epidemic potential. *PLoS pathogens*
633  3:e201.

634

635 Vega-Rúa A, Zouache K, Girod R, Failloux A-B, and Lourenço-de-Oliveira R. 2014. High level
636  of vector competence of Aedes aegypti and Aedes albopictus from ten American
637  countries as a crucial factor in the spread of Chikungunya virus. *Journal of virology*
638  88:6294-6306.

639

640 Yamane D, McGivern DR, Wauthier E, Yi M, Madden VJ, Welsch C, Antes I, Wen Y, Chugh
641  PE, and McGee CE. 2014. Regulation of the hepatitis C virus RNA replicase by
642  endogenous lipid peroxidation. *Nature medicine* 20:927-935.

643

644 Yang J, Yan R, Roy A, Xu D, Poisson J, and Zhang Y. 2015. The I-TASSER Suite: protein
645  structure and function prediction. *Nature methods* 12:7-8.

646

647 Zandi K, Teoh B-T, Sam S-S, Wong P-F, Mustafa MR, and AbuBakar S. 2011. Antiviral activity
648  of four types of bioflavonoid against dengue virus type-2. *Virology journal* 8:1.

649

650 Zhang Y. 2008. I-TASSER server for protein 3D structure prediction. *BMC bioinformatics* 9:40.

651

Parameters used for molecular docking of hesperetin with each protein of interest.

All grid boxes with spacing size of 1.000 Å have sufficient sizes to cover the entire protein structures during molecular docking.

Proteins	Center-X	Center-Y	Center-Z	Size-X	Size-Y	Size-Z
Nsp1	8.490	-21.201	-6.330	96	78	70
3TRK	11.569	24.420	21.707	52	76	56
3GPG	8.490	-21.201	-21.201	96	78	70
NsP4	76.026	77.432	77.204	78	84	58
SPK2	67.704	77.970	71.232	72	72	68

Binding energies between hesperetin and different types of proteins.

The energies involved in each ligand-receptor interaction was analysed using the Discovery Studio 2.5.

Proteins	Electrostatic Interaction Energy (kcal/mol)	Van der Waals Interaction Energy (kcal/mol)	Interaction Energy (kcal/mol)
NsP1	16.785	-29.699	-12.914
3TRK	-454.598	-83.186	-537.784
3GPG	-405.273	-129.780	-535.053
NsP4	-32.689	-28.904	-61.594
SPK2	14.815	-27.477	-12.663

Hydrogen bonding between hesperetin and CHIKV nsP1.

This table documents the residues involved in the hydrogen bond formation as well as the angle DHA and length of the hydrogen bonds as analysed using the Discovery Studio 2.5. The binding affinities as ranked by the AutoDock Vina 1.5.6 are recorded in the final column of the table.

Hydrogen bonds	Angle DHA (°)	Distance (Å)	Binding Affinity (kcal/mol)
Hesperetin:UNK1:H2 – nsP1:ASP310:OD1	167.07°	1.66709	-7.6
nsP1:GLY311:HN – Hesperetin:UNK1:O19	159.57°	2.13746	
nsP1:ARG365:HH21 – Hesperetin:UNK1:O20	93.9791°	2.49524	
nsP1:ARG365:HH22 – Hesperetin:UNK1:O20	104.508°	2.33411	
nsP1:ARG365:HH22 – Hesperetin:UNK1:O21	121.423°	2.29742	
Hesperetin:UNK1:H1 – nsP1:HIS45:ND1	149.472°	2.28058	-7.5
nsP1:GLY190:HN – Hesperetin:UNK1:O20	124.29°	2.43961	
Hesperetin:UNK1:H1 – nsP1:ASP36:OD2	125.798°	2.08242	-7.4
Hesperetin:UNK1:H2 – nsP1:PRO68:O	146.956°	2.24366	
nsP1:ARG71:HH11 – Hesperetin:UNK1:O20	158.052°	2.07172	
Hesperetin:UNK1:H3 – nsP1:GLU129:O	119.206°	2.47249	
nsP1:LEU108:HN – Hesperetin:UNK1:O20	153.395°	2.33121	
nsP1:LEU135:HN – Hesperetin:UNK1:O17	125.791°	2.08609	
nsP1:ARG70:HN – Hesperetin:UNK1:O17	134.179°	2.09364	-7.3
nsP1:ARG252:HH12 – Hesperetin:UNK1:O20	171.884°	2.30037	
Hesperetin:UNK1:H1 – nsP1:ASP448:OD1	154.403°	1.82012	-7.2
Hesperetin:UNK1:H3 – nsP1:VAL475:O	159.829°	1.84851	
Hesperetin:UNK1:H3 – nsP1:SER44:OG	119.912°	2.48095	-6.9
nsP1:ARG71:HH12 – Hesperetin:UNK1:O20	126.228°	2.28728	

Hydrogen bonding between hesperetin and 3TRK.

This table documents the residues involved in the hydrogen bond formation as well as the angle DHA and length of the hydrogen bonds as analysed using the Discovery Studio 2.5. The binding affinities as ranked by the AutoDock Vina 1.5.6 are recorded in the final column of the table.

Hydrogen bonds	Angle DHA (°)	Distance (Å)	Binding Affinity (kcal/mol)
Hesperetin:UNK1:H3 – 3TRK:ASP1246:OD1	132.214	2.19274	-6.9
3TRK:TRP1084:HE1 – Hesperetin:UNK1:O18	140.389	2.20564	
3TRK:TRP1084:HE1 – Hesperetin:UNK1:O19	148.713	2.13609	
Hesperetin:UNK1:H3 – 3TRK:Ser1048:OG	144.592	2.32087	-6.8
Hesperetin:UNK1:H1 – 3TRK:GLN1241:O	93.425	2.48789	-6.6
3TRK:ALA1180:HN – Hesperetin:UNK1:O20	136.259	2.09817	-6.5
3TRK:LYS1091:HZ2 – Hesperetin:UNK1:O18	134.881	2.44139	
3TRK:ARG1267:HH12 – Hesperetin:UNK1:O19	141.467	2.27262	-6.4
3TRK:ARG1267:HH22 – Hesperetin:UNK1:O19	149.413	2.06422	
Hesperetin:UNK1:H1 – 3TRK:LEU1065:O	144.638	2.23416	
3TRK:PHE1225:HN – Hesperetin:UNK1:O10	145.498	2.33505	
3TRK:ASN1135:HN – Hesperetin:UNK1:O18	126.233	2.487381	-6.1
3TRK:ASN1135:HN – Hesperetin:UNK1:O19	129.610	2.38619	

Hydrogen bonding between hesperetin and 3GPG.

This table documents the residues involved in the hydrogen bond formation as well as the angle DHA and length of the hydrogen bonds as analysed using the Discovery Studio 2.5. The binding affinities as ranked by the AutoDock Vina 1.5.6 are recorded in the final column of the table.

Hydrogen bonds	Angle DHA (°)	Distance (Å)	Binding Affinity (kcal/mol)
Hesperetin:UNK1:H1 – 3GPG:TYR142:O	123.476	1.97816	-8.5
3GPG:LEU108:HN – Hesperetin:UNK1:O17	162.843	2.17416	
3GPG:SER110:HN – Hesperetin:UNK1:O20	145.746	2.0736	
3GPG:VAL33:HN – Hesperetin:UNK1:O20	125.205	2.35031	-8.3
3GPG:ARG144:HN – Hesperetin:UNK1:O19	159.099	1.95421	
Hesperetin:UNK1:H2 – 3GPG:GLU17:O	165.815	1.93615	-7.3
3GPG:THR122:HN – Hesperetin:UNK1:O	145.209	2.13631	
3GPG:ASN72:HD22 – Hesperetin:UNK1:O20	139.167	2.03974	
3GPG:SER110:HN – Hepseretin:UNK1:O21	152.590	1.95709	-7.0
3GPG:TRP41:HE1 – Hesperetin:UNK1:O18	123.985	2.27795	
3GPG:LYS7:HZ2 – Hesperetin:UNK1:O20	144.885	2.15643	
Hesperetin:UNK1:H3 – 3GPG:TYR4:O	148.477	2.16364	-6.9
3GPG:GLN157:HE22 – Hesperetin:UNK1:O20	129.097	2.30335	
Hesperetin:UNK1:H1 – 3GPG:GLY116:O	128.866	2.03758	
Hesperetin:UNK1:H2 – 3GPG:GLU17:OE2	128.230	2.31651	
3GPG:ARG120:HH21 – Hesperetin:UNK1:O17	123.759	2.34233	
3GPG:LEU108:HN – Hesperetin:UNK1:O17	178.542	1.72039	

Hydrogen bonding between hesperetin and CHIKV nsP4.

This table documents the residues involved in the hydrogen bond formation as well as the angle DHA and length of the hydrogen bonds as analysed using the Discovery Studio 2.5. The binding affinities as ranked by the AutoDock Vina 1.5.6 are recorded in the final column of the table.

Hydrogen bonds	Angle DHA (°)	Distance (Å)	Binding Affinity (kcal/mol)
nsP4:GLN364:HE22 – Hesperetin:UNK1:O21	148.552	2.20397	-7.7
nsP4:ARG374:HH21 – Hesperetin:UNK1:O19	121.976	2.4414	
Hesperetin:UNK1:H3 – nsP4:ALA104:O	127.732	2.19555	-7.6
Hesperetin:UNK1:H1 – nsP4:ALA103:O	147.014	1.88423	-7.5
nsP4:GLY190:HN – Hesperetin:UNK1:O20	123.296	2.41584	-7.4
Hesperetin:UNK1:H2 – nsP4:ARG110:O	117.610	2.16176	
nsP4:LEU108:HN – Hesperetin:UNK1:O20	147.895	2.27281	
nsP4:LEU135:HN – Hesperetin:UNK1:O17	126.767	2.09964	
Hesperetin:UNK1:H1 – nsP4:THR437:O	111.885	2.2692	
Hesperetin:UNK1:H2 – nsP4:ASP479:OD1	108.572	2.17349	
nsP4:THR437:HN – Hesperetin:UNK1:O17	174.240	2.08043	
nsP4:LEU180:HN – Hesperetin:UNK1:O19	117.866	2.47914	

Hydrogen bonding between hesperetin and SPK2.

This table documents the residues involved in the hydrogen bond formation as well as the angle DHA and length of the hydrogen bonds as analysed using the Discovery Studio 2.5. The binding affinities as ranked by the AutoDock Vina 1.5.6 are recorded in the final column of the table.

Hydrogen bonds	Angle DHA (°)	Distance (Å)	Binding Affinity (kcal/mol)
SPK2:ARG227:HE – Hesperetin:UNK1:O21	132.729	2.39668	-7.7
Hesperetin:UNK1:H3 – SPK2:ALA431:O	106.199	2.32194	
SPK2:GLN223:HE – Hesperetin:UNK1:O19	111.042	2.45074	-7.6
SPK2: GLN625:HN – Hesperetin:UNK1:O17	110.511	2.45589	
Hesperetin:UNK1:H1 – SPK2:GLU624:OE1	139.804	2.27908	
Hesperetin:UNK1:H2 – SPK2:ARG373:O	129.174	1.92199	
Hesperetin:UNK1:H3 – SPK2:ASP342:OD1	141.848	2.21488	
SPK2:ARG227:HE – Hesperetin:UNK1:O21	130.540	2.3656	-7.5
Hesperetin:UNK1:H2 – SPK2:GLN625:O	130.888	1.94553	
Hesperetin:UNK1:H3 – SPK2:ALA431:O	105.734	2.29542	
SPK2:ASP110:HN – Hesperetin:UNK1:O17	152.041	2.32426	-7.4
Hesperetin:UNK1:H1 – SPK2:CYS100:O	138.862	2.43301	
Hesperetin:UNK1:H2 – SPK2:ARG373:O	120.303	2.05193	-7.3
Hesperetin:UNK1:H3 – SPK2:ASP342:OD1	147.571	2.13992	
SPK2:GLY248:HN – Hesperetin:UNK1:O19	134.859	2.21696	-7.1
Hesperetin:UNK1:H1 – SPK2:CYS276:O	89.142	2.41654	
Hesperetin:UNK1:H1 – SPK2:THR641:OG1	135.818	2.17768	-7.0

Pi-interactions between hesperetin and respective proteins.

The residues involved and length of each pi-interaction as well as the types of pi-interactions formed were analysed using the Discovery Studio 2.5.

Protein	Binding	Distance (Å)	Interaction
NsP1	Hesperetin:UNK1 – ARG70:NE	5.2141	Pi-Cation
	Hesperetin:UNK1 – nsP1:TYR185	6.18796	Pi-Pi
	Hesperetin:UNK1 – nsP1:ARG252:NE	6.85892	Pi-Cation
	Hesperetin:UNK1 – ARG252:NE	6.0649	Pi-Cation
	Hesperetin:UNK1 – nsP1:PHE43	6.334	Pi-Pi
	Hesperetin:UNK1 – nsP1:LYS442:NZ	5.9124	Pi-Cation
3TRK	Hesperetin:UNK1 – 3TRK:TYR1079	4.72556	Pi-Pi
	Hesperetin:UNK1 – 3TRK:TYR1079	5.65846	Pi-Pi
	Hesperetin:UNK1 – 3TRK:TYR1177	4.36635	Pi-Pi
	Hesperetin:UNK1 – 3TRK:PHE1225:HB2	2.74925	Pi-Sigma
3GPG	Hesperetin: UNK1 – 3GPG:TRP148	5.10212	Pi-Pi
	Hesperetin: UNK1 – 3GPG:TRP148	4.15778	Pi-Pi
	Hesperetin:UNK1 – 3GPG:LYS118:NZ	3.86706	Pi-Cation
	Hesperetin:UNK1 – 3GPG:GLY30:HA1	2.84749	Pi-Sigma
	Hesperetin:UNK1 – 3GPG:VAL113:HB	2.9202	Pi-Sigma
	Hesperetin:UNK1- 3GPG:TYR63	4.02708	Pi-Pi
	3GPG:TRP148 – Hesperetin:UNK1	4.22731	Pi-Pi
	3GPG:TRP148 – Hesperetin:UNK1	4.05885	Pi-Pi
NsP4	Hesperetin:UNK1 – nsP4:ARG374:NE	5.53545	Pi-Cation
	Hesperetin:UNK1 – nsP4:ARG70:NE	5.3946	Pi-Cation
	Hesperetin:UNK1 – nsP4:ARG70:NE	6.64674	Pi-Cation
	Hesperetin:UNK1 – nsP4:ARG70:NE	5.65215	Pi-Cation

	Interaction	Distance	Type
	Hesperetin:UNK1 – nsP4:ARG70:NE	5.28131	Pi-Cation
	Hesperetin:UNK1 – nsP4:TYR22	4.15499	Pi-Pi
	Hesperetin:UNK1 – nsP4:ARG70:NE	4.49028	Pi-Cation
	Hesperetin:UNK1 – nsP4:TYR185	6.16947	Pi-Pi
	Hesperetin:UNK1 – nsP4:ARG70:NE	5.20374	Pi-Cation
	Heesperetin:UNK1 – nsP4:ARG70:NE	4.51522	Pi-Cation
	Hesperetin:UNK1 – nsP4:ARG70:HD1	2.61933	Pi-Sigma
SPK2	Hesperetin:UNK1 – SPK2:TYR372	4.91884	Pi-Pi
	SPK2:TYR372 – Hesperetin:UNK1	4.34443	Pi-Pi
	Hesperetin:UNK1 – SPK2:ARG351:NE	6.2923	Pi-Cation

Lipinski's values of the hesperetin molecule designed for this study and that of the available data from PubChem.

A compound with drug-likeness properties should possess molecular weight less than 500 g/mol, Log P less than 5, less than 5 H-bond donors, less than 10 H-bond acceptors and molar refractivity in the range of 40-130.

Criteria	From the present study	Extracted from PubChem
Molecular weight (g/mol)	302.00	302.28
H-bond donors	3	3
H-bond acceptors	6	6
Log-P	2.5	2.4
Molar refractivity	76.75	76.93

Relative binding free energies of complexes estimated using MM-GBSA.

Note: The EEL and vdW represent the electrostatic and van der Waals contributions from MM, respectively. EGB stands for GB electrostatic contribution to the solvation free energy, and ESURF is the nonpolar contribution to the solvation free energy. $\Delta E_{binding}$ (in kcal mol^{-1}, binding energy neglecting the contribution of entropy) is the final estimated binding free energy calculated from the terms above.

Complex	EEL	vdW	EGB	ESURF	$\Delta E_{binding}$
3GPG + hesperetin	-10.26	-36.62	23.47	-4.76	-28.18
3TRK + hesperetin	-4.13	-28.32	18.61	-3.61	-17.46

Figure 1

The binding positions with the highest binding affinities of hesperetin (yellow ball and stick structure) when docked against different proteins (flat ribbon coloured from N-to-C terminal).

(A) nsP1 with binding affinity of -7.6 kcal/mol, (B) 3TRK with binding affinity of -6.9 kcal/mol, (C) 3GPG with binding affinity of -8.5 kcal/mol, (D) nsP4 with binding affinity of -7.7 kcal/mol, (E) SPK2 with binding affinity of -7.7 kcal/mol
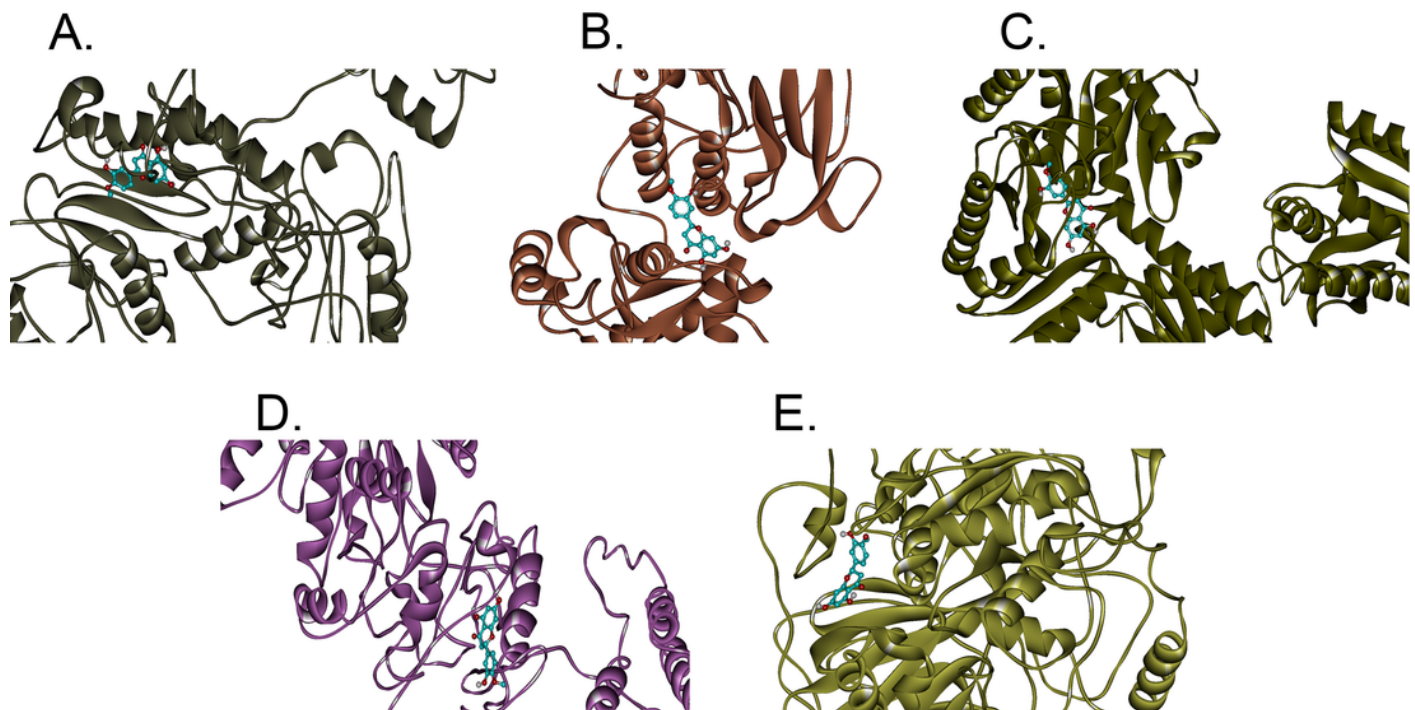
Figure 2

2D diagram of interaction between hesperetin and nsP1.

The diagram shows the ligand-receptor interactions and close amino acid residues found in the binding pocket.
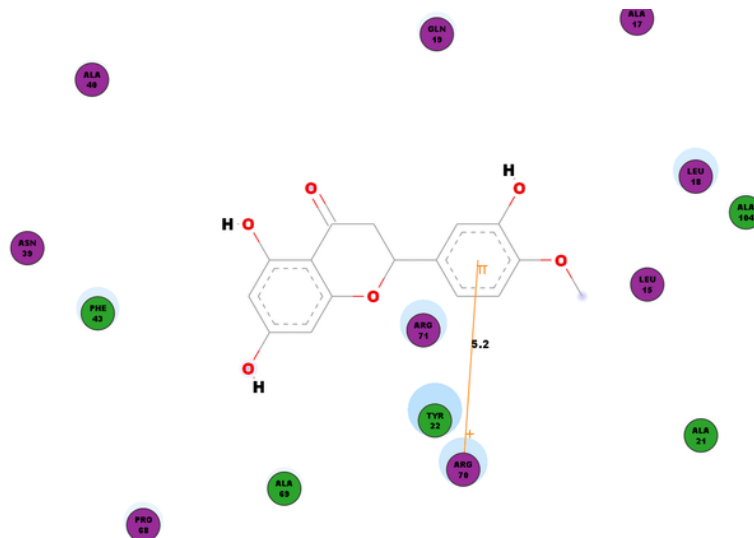
Figure 3

2D diagram of interaction between hesperetin and 3TRK.

The diagram demonstrates the ligand-receptor interactions and close amino acid residues found in the binding pocket.
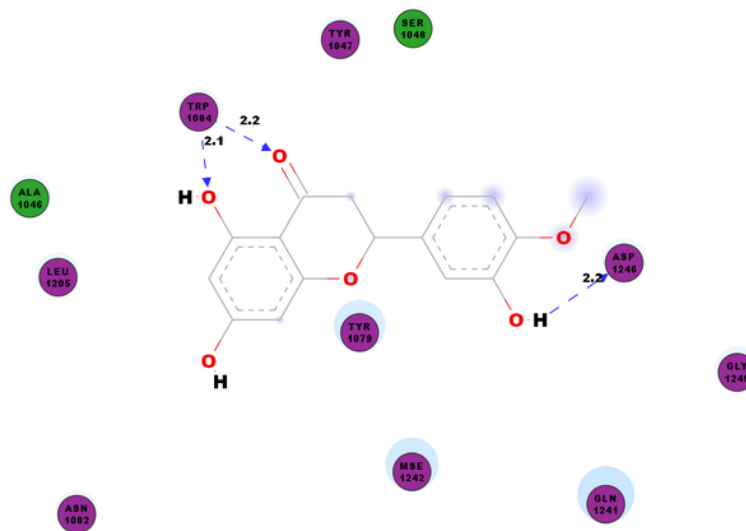
Figure 4

2D diagram of interaction between hesperetin and 3GPG.

The diagram illustrates the ligand-receptor interactions and close amino acid residues found within the binding pocket.
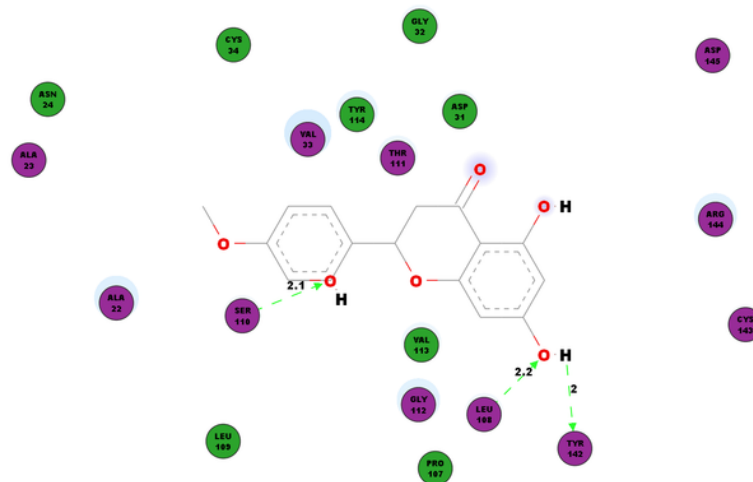
Figure 5

2D diagram of interaction between hesperetin and nsP4.

The diagram shows the ligand-receptor interactions and close amino acid residues found in the binding pocket.

Figure 6

2D diagram of interaction between hesperetin and SPK2.

The diagram demonstrates the ligand-receptor interactions and close amino acid residues found in the binding pocket.
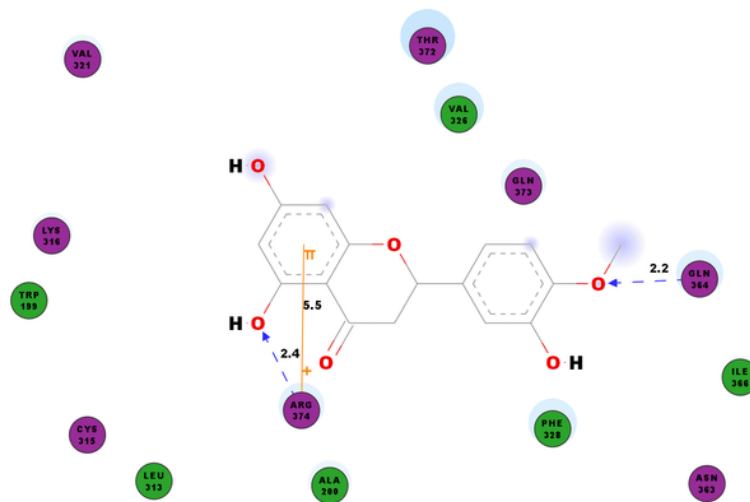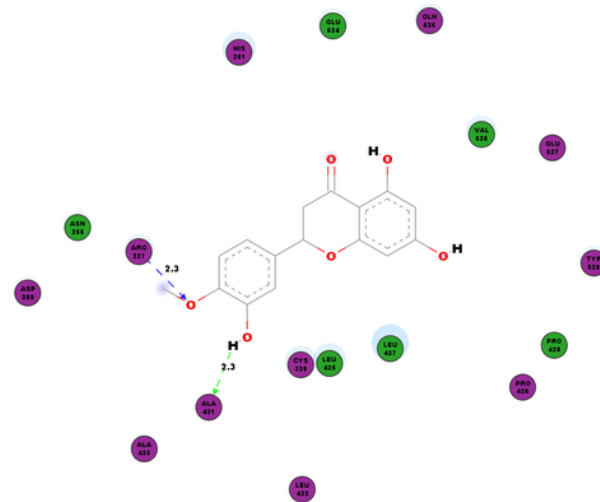
Figure 7

Time series of RMSD from the minimized starting structure calculated using the backbone atoms of the protein.

RMSD computed with respect to the minimized starting structure is less than 1.8 Å , hence showing that the simulated systems are well equilibrated and do not deviate much from the initial starting structure.
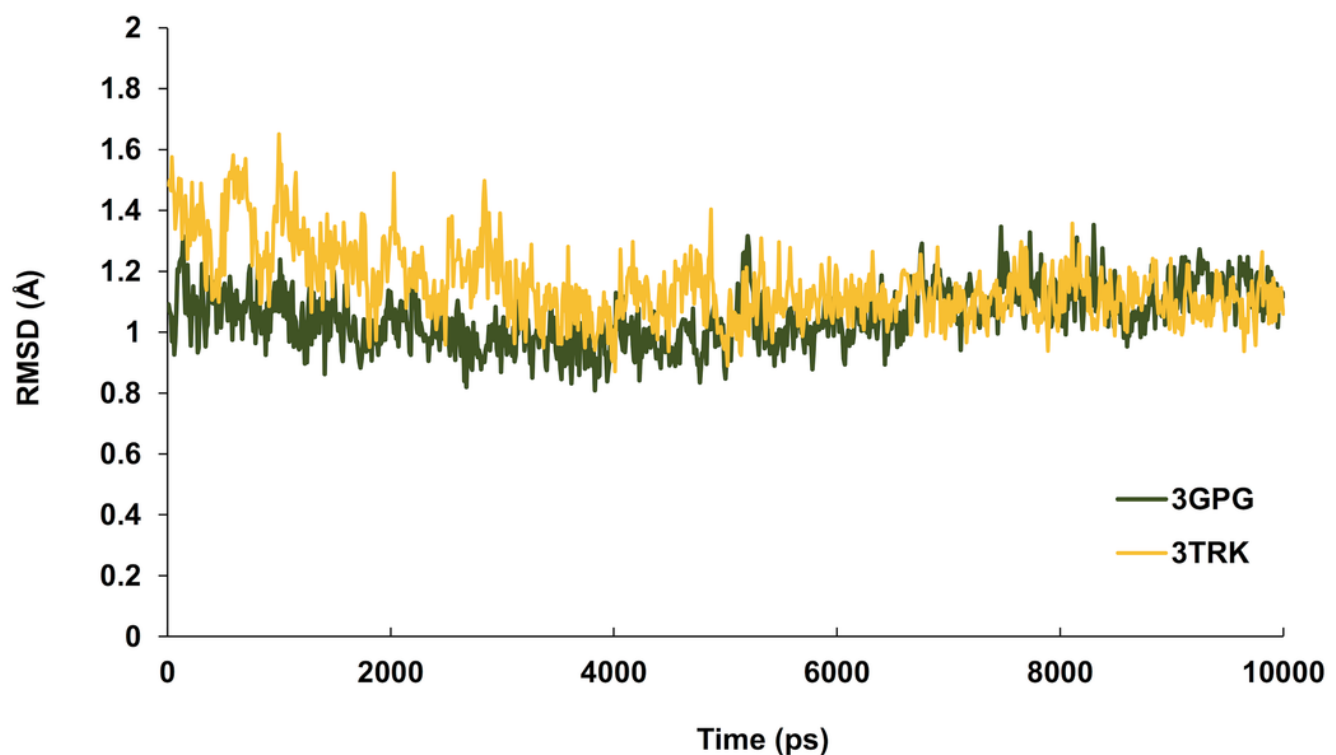
Figure 8

Lowest energy structure of ligand-receptor complexes.

A. 3GPG and **B. 3TRK** in complexed with hesperetin (shown in stick representation, only polar hydrogen is shown). Both complexes remained stable throughout the 10 ns simulations.